

Interactive comment on “Observations of the scale-dependent turbulence and evaluation of the flux-gradient relationship for sensible heat for a closed Douglas-Fir canopy in very weak wind conditions” by D. Vickers and C. Thomas

D. Vickers and C. Thomas

vickers@coas.oregonstate.edu

Received and published: 1 July 2014

[12pt]article

epsfig graphics

C4313

1 Response to reviewer 2

We agree that we present some observations for which we have no physical explanation and therefore can only speculate about. Clearly, there is much to learn about the details of the spectra and co-spectra of turbulence quantities, especially within and below the forest canopy.

The first point is "the peak at very small timescales observed in the subcanopy". We must assume that the reviewer is referring to the peak in the double-peaked vertical velocity spectra at 0.8 s during the day. As we stated in the paper, the double peak structure may be associated with tree stem wake, although we have no direct measurements to confirm this. We are not aware of any previous study showing a double peak in the subcanopy vertical velocity spectra. The fact that the double peak is observed for all wind directions gives some confidence that the result is not due to a measurement problem. The same double peak is observed for the heat flux. As suggested by the reviewer, the formation of a double peak in the vertical velocity spectra may be related to canopy density. The canopy studied here is remarkable for its large plant area index of 9.4. Our previous study in 2013 AgForMet looked at a tall open canopy ponderosa pine site with a plant area index of 3.4. No double peak in the vertical velocity spectra was detected in the subcanopy of the tall open canopy site.

The second point is the "somewhat similar time scale of the turbulence maximum between the different levels". With no canopy or large z/h , the timescale associated with the peak in the vertical velocity spectra increases with height, presumably due to the increased obstruction or blocking action to the flow as the observational level approaches the surface. However, the situation is more complicated for small z/h . Seginer et al., 1976 (*Boundary Layer Met.*, 10, 423-453) found that the peak frequency of the turbulence in plant canopies seemed to be independent of height.

The third point is the unusually large values of the turbulence intensity inside the canopy, which the reviewer suggested may be a factor in the unusually large estimates

C4314

of the exchange coefficient above the canopy; however, we have no direct evidence to support that claim. We are not aware of any previous study finding values of the turbulence intensity as large as found here, possibly due in part to the lack of high quality turbulence measurements collected inside canopies.

We did include the vertical velocity variance in the Tables.

Comment I.1 p.11937: We have removed the sentence.

Comment I.7 p.11938: We are unaware of any references discussing why the canopy might inhibit horizontal motions more than vertical ones. It is difficult to explain this behavior. Our speculation is that motions generated aloft and moving downward through the canopy are somehow selectively suppressed by the spacing of the canopy elements, resulting in large values of VAR.

Comment I.13-15 p.11941: CH is positively related to the vertical velocity variance; however, models do not have information on the vertical velocity variance, so developing relationships between the variance and CH may not be useful to parameterize the flux.

As requested, we have added a new panel to Fig 7 showing the scatter plot for the 38-m level.

The reviewer notes that in the subcanopy... "where similarity theory is known to fail"; however, our results support the bulk flux approach in the subcanopy, even with very small fluxes and very weak winds.

Regarding the large estimate of CH above the canopy, the reviewer makes a good point that we did not mention; roughness sublayer effects. If the 38-m measurements are indeed in the roughness sublayer, then the turbulence and the fluxes may be heterogeneous in the horizontal and much larger than predicted by standard flux gradient relationships, even for long time averages, adding considerable uncertainty to our results. Baldocchi and Hutchison 1988 (Boundary-Layer Met., 42, 293-311) reported

C4315

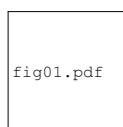


Fig. 1. The frequency distribution of the subcanopy mean wind speed (top) and the standard deviation of vertical velocity (bottom).



Fig. 2. Composites of three levels of daytime vertical velocity spectra wv ($m^2 s^{-2}$, left column), kinematic heat flux cospectra wT ($^{\circ}C m s^{-1}$, middle column), and the along- and cross-wind (red) components of the momentum flux (wu and wv) ($m^2 s^{-2}$, right column). All quantities have been multiplied by one-thousand. The error bars denote the 99% confidence limit about the mean. The vertical line in each panel denotes $\tau = 20$ s.

small heterogeneity of the turbulence velocity spectra in the subcanopy of an almond orchid. That is, roughness sublayer effects were small in the orchid subcanopy.

Our presentation of CH for the "single-source" approach was done as an exercise for demonstration purposes. We are not aware which models may be employing a single-source approach for grid points with tall forest canopies. Although our result may be obvious to most researchers, we feel that it is worth the 4 sentences and 1 Fig devoted to it.

We include all figures below.

C4316



Fig. 3. Same as Figure 2 except for nighttime.



Fig. 4. Three levels of the scale-dependence of the velocity aspect ratio VAR. The vertical line denotes $\tau = 20$ s.

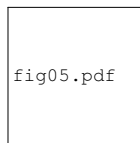


Fig. 5. The normalized turbulence intensity at three levels as a function of the wind speed above the canopy. Error bars denote \pm one standard error.

C4317

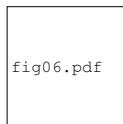


Fig. 6. The observed diurnal cycle of the subcanopy sensible heat flux with standard error bars (top) and \pm one standard deviation (bottom), where the uncertainty is due to the day-to-day variability in the heat flux for a given hour of the day over the entire 5-month period.

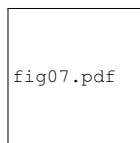


Fig. 7. Scatter plot of the 30-minute average subcanopy kinematic heat flux (lower panel) as a function of the product of the mean wind speed and the temperature difference. The slope of the linear regression line (red) is an estimate of the subcanopy Stanton number (C_H). The estimate for the subcanopy C_H using this approach is $1.1 \pm 0.04 \times 10^{-3}$, using a 90% confidence interval for the slope, and the regression explains 32% of the variance. Above the canopy at 38 m (upper panel), the estimate of the Stanton number is $73.5 \pm 1.3 \times 10^{-3}$, with 77% of the variance explained.

C4318



fig08.pdf

Fig. 8. The frequency distribution of the subcanopy Stanton number (multiplied by one-thousand) where each 30-minute estimate is computed as the heat flux divided by the product of the mean wind speed and the temperature difference. This approach for estimating the Stanton number yields a mean value of 1.1×10^{-3} and a standard deviation of 2.05×10^{-3} .



fig09.pdf

Fig. 9. The kinematic heat flux as a function of the product of the mean wind speed and the temperature difference at 38 m (top panel) and at 4 m (bottom). The slopes of the linear regression lines (red) are estimates of the Stanton number: $73.5 \pm 1.3 \times 10^{-3}$ at 38 m, and $1.1 \pm 0.04 \times 10^{-3}$ at 4 m. Each of the ten class averages contains an equal number (282) of 30-minute samples. Error bars denote \pm one standard error.

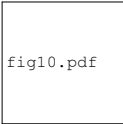


fig10.pdf

Fig. 10. The frequency distribution (top panel) and the diurnal cycle (bottom) of the above canopy Stanton number multiplied by one-thousand. Error bars denote \pm one standard error.

C4319




fig11.pdf

Fig. 11. The kinematic heat flux as a function of the product of the mean wind speed and the temperature difference using the single source approach (see text). The slope of the linear regression line (red) is estimate of the Stanton number: $-12.8 \pm 27.9 \times 10^{-3}$. Each of the ten class averages contains an equal number (282) of 30-minute samples. Error bars denote \pm one standard error.

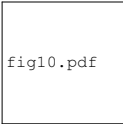


fig10.pdf

Fig. 12. The frequency distribution (top panel) and the diurnal cycle (bottom) of the above canopy Stanton number multiplied by one-thousand. Error bars denote \pm one standard error.




fig11.pdf

Fig. 13. The kinematic heat flux as a function of the product of the mean wind speed and the temperature difference using the single source approach (see text). The slope of the linear regression line (red) is estimate of the Stanton number: $-12.8 \pm 27.9 \times 10^{-3}$. Each of the ten class averages contains an equal number (282) of 30-minute samples. Error bars denote \pm one standard error.

C4320




fig10.pdf

Fig. 14. The frequency distribution (top panel) and the diurnal cycle (bottom) of the above canopy Stanton number multiplied by one-thousand. Error bars denote \pm one standard error.




fig11.pdf

Fig. 15. The kinematic heat flux as a function of the product of the mean wind speed and the temperature difference using the single source approach (see text). The slope of the linear regression line (red) is estimate of the Stanton number: $-12.8 \pm 27.9 \times 10^{-3}$. Each of the ten class averages contains an equal number (282) of 30-minute samples. Error bars denote \pm one standard error.